Macromolecules **1992,** *25,* 2359–2368

Interfacial Segment Density Profiles of End-Anchored Polymers in a Melt†

Richard A. L. Jones

Department of Physics, Cambridge University, Cambridge CB3 0HE, U.K.

Laura J. Norton, Kenneth R. Shull, and Edward J. Kramer*

Department of Materials Science and Engineering and the Materials Science Center,
Cornell University, Ithaca, New York 14853

Gian P. Felcher and Alamgir Karim

Materials Science Division, Argonne National Laboratory, Argonne, Illinois 60439-4814

Lewis J. Fetters

Exxon Research and Engineering Company, Route 22 East, Annandale, New Jersey 08801

Received July 8, 1991; Revised Manuscript Received November 13, 1991

ABSTRACT: The segment density profile of end-functionalized deuterated polystyrene (EF-dPS) polymers anchored in a surrounding melt of hydrogenated polystyrene (hPS) to an interface with silicon was determined by neutron reflectometry. Thin films of mixtures with various volume fractions of the EF-dPS and hPS were spun cast from toluene solutions onto the silicon. These films as cast were uniform as a function of depth. After heating to 184 °C for approximately 1 day to allow equilibrium segregation to be achieved in the films, neutron reflection measurements were performed. The EF-dPS segment density profiles $\phi(z)$ needed to fit the reflectivity data showed a high ϕ at the silicon interface which increased to a maximum approximately 10 nm away from the interface and then fell monotonically to the bulk segment density ϕ_∞. The interface excess determined by integration of these profiles was in excellent agreement with that directly determined by forward recoil spectrometry on the same samples. The form of the profiles is consistent with the predictions of a self-consistent mean field theory if, in addition to a large attachment free energy of the end group to the silicon, there is a weak preferential attraction of the silicon for the more polarizable hPS segments relative to the less polarizable dPS segments.

1. Introduction

Adsorption of polymer chains from solution to surfaces or interfaces has long been the subject of intense study.[1,2] The related problem of adsorption of chains to a surface or interface from a melt is now also beginning to receive attention.[3–7] Such phenomena are expected on rather general grounds to be widespread and of great practical importance in areas such as interphase adhesion in composite materials and the control of surface properties. Polymer blends have very low entropies of mixing compared to polymer solutions, so one expects large surface effects from relatively small perturbations. Previous work, for example, has shown that the isotopic surface energy difference between deuterated polystyrene (dPS) and protonated polystyrene (hPS) can be sufficient to cause substantial adsorption to the air surface of dPS/hPS blends.[4,7] In this work we demonstrate, using neutron reflectivity and forward recoil spectrometry, that a small end group is sufficient to drive substantial adsorption of dPS from a blend of the end-functionalized dPS and conventionally terminated hPS to an interface with a silicon substrate; using neutron reflectivity we are able to measure the segment density profile near the interface.

2. Experimental Section

The perdeuteriopolystyrene was prepared using the vacuum line practices outlined elsewhere.[8] The initiator was purified *sec*-butyllithium with benzene at 25 °C as the solvent. Termination was carried out by exposing the living polymer in solution first to a small amount of butadiene, designed to give 3–5 units of butadiene at the chain end, and then to purified trimethylchlorosilane. This procedure yielded the polymer schematically shown in Figure 1.

Characterization was done using a combination of low-angle laser light scattering (Chromatix KMX-6) and size exclusion chromatography. The former yielded $M_w = 250\,000$ and the latter yielded heterogeneity indices of 1.05 for M_z/M_w and 1.06 for M_w/M_n. Hydrogenated (normal) polystyrene of weight-average molecular weight 575 000 and polydispersity index 1.06 was purchased from Pressure Chemical Co. Solutions of blends of the end-functionalized deuterated polystyrene with normal polystyrene in toluene were spun onto 2-in.-diameter, $^3/_{16}$-in.-thick polished silicon wafers, from which the native oxide had previously been removed by etching in a buffered hydrofluoric acid solution. These samples were then annealed under vacuum at 184 °C for times between 20 and 50 h.

Measurements of neutron reflectivity were carried out using the POSY II reflectometer at IPNS, Argonne National Laboratory. The technique and this instrument in particular are described in detail below.

Forward recoil spectrometry (FRES) measurements of the deuterium depth profile were carried out using an incident beam of 3.4-MeV He^{2+} ions, as described elsewhere.[4,9–11]

3. Neutron Reflectivity

When neutrons propagate through a medium in which the scattering centers are small compared to the wavelength of the neutrons, the effect of the medium may be

---

† Report No. 7179 issued by the Materials Science Center.

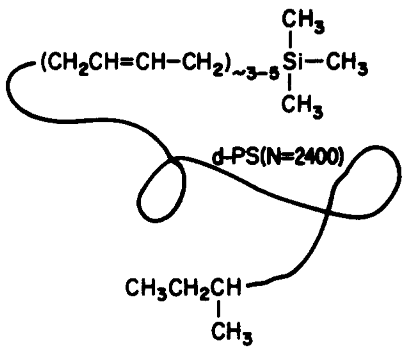

Figure 1. Chemical structure of the end group.

represented by a smooth pseudopotential whose magnitude is related simply to the total scattering length density of the material as

$$V_{\text{eff}} = \frac{2\pi\hbar^2}{m}\frac{b}{V} \tag{1}$$

where b is the sum of all the scattering lengths in a volume V.[12,13] Thus the neutrons obey the Schrödinger equation

$$-\left(\frac{\hbar^2}{2m}\right)\nabla^2\psi + V\psi = E\psi \tag{2}$$

If the potential is a function only of z, that is to say if it is purely one-dimensional, the equation may be separated; the equation for the direction parallel to the plane corresponds to free motion and the parallel component of the wavevector is constant. The perpendicular component of the motion then obeys a one-dimensional Schrödinger equation

$$-\left(\frac{\hbar^2}{2m}\right)\left(\frac{d^2\psi}{dz^2}\right) + V\psi = E\psi \tag{3}$$

where $E = (\hbar^2k^2/2m)$, where k is the perpendicular component of the wavevector of the incoming beam. This may be solved to give the amplitude reflectance r and the reflectivity $R = |r|^2$. For neutrons propagating from vacuum into a uniform material of scattering length density (b/V) the perpendicular component of the wavevector within the material k_i is given by

$$k_i = (k^2 - 4\pi(b/V))^{1/2} \tag{4}$$

For $4\pi(b/V) > k^2$ this quantity is imaginary; the neutrons propagate into the material only as an evanescent wave, giving rise to total external reflection; i.e., the reflectivity is unity. If $4\pi(b/V) < k^2$ and the interface between the vacuum and the medium is sharp, then the reflectivity is given by the Fresnel expression[14]

$$R = |r|^2 = \left(\frac{k - k_i}{k + k_i}\right)^2 \tag{5}$$

which has the limiting form at high k of

$$R \approx \pi^2(b/V)^2k^{-4} \tag{6}$$

If the interface is rough or graded, the reflectance of such an interface is given by the formula

$$r_D = r_{\text{Fresnel}} \exp(-2kk_iD^2) \tag{7}$$

where D is the Gaussian width of the interface.[15]

The reflectivity of a multilayer stack of thin slabs may be calculated by the following recursive scheme.[14] Consider the multilayer illustrated in Figure 2, in which the perpendicular component of the wavevector in layer i is k_i and the thickness of layer i is d_i. The reflectance of an individual interface between layers i and $i - 1$ may be denoted $r_{i-1,i}$ and is given by the Fresnel expression

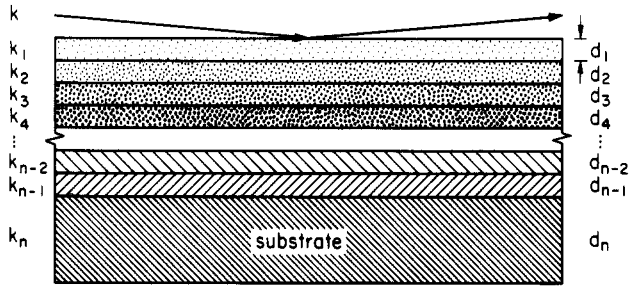

Figure 2. A schematic multilayer structure, with layers of thickness d_i in which the perpendicular component of the neutron wavevector is k_i.

$$r_{i,i-1} = \frac{k_{i-1} - k_i}{k_{i-1} + k_i} \tag{8}$$

The combined reflectance of the interfaces between the substrate and layer $n - 1$, and layer $n - 1$ and $n - 2$, denoted $r_{n-2,n}$, can be formed from the reflectances of these individual interfaces:

$$r_{n-2,n} = \frac{r_{n-2,n-1} + r_{n-1,n}\exp(2ik_{n-1}d_{n-1})}{1 + r_{n-2,n-1}r_{n-1,n}\exp(2ik_{n-1}d_{n-1})} \tag{9}$$

Now we can combine this reflectance with the reflectance of the interface between layers $n - 3$ and $n - 2$ to yield the reflectance of all interfaces from $n - 3$ to the substrate. This process is now continued recursively until the top interface is reached.

This algorithm may be conveniently and compactly programmed and forms the basis of the computer program LAYERS which is in use at IPNS. By approximating a continuous profile by a stack of such thin layers (typically one chooses layer thicknesses to give a constant increment in scattering length density between each layer) one may calculate the reflectivity of any profile to the accuracy required within a given k range. It is instructive, however, to write down the continuum limit of this expression:

$$r(0) = -\int_0^\infty \frac{dk(z)}{dz}\frac{1 - r(z)^2}{2k(z)}\exp\{-2i\int_0^z k(z')\,dz'\}\,dz \tag{10}$$

It is not obvious that this highly nonlinear transform can be inverted in the absence of any phase information, but it takes a simpler form in the limit of high k:

$$r(0) = \frac{\pi}{k^2}\int_0^\infty \frac{d(b/V)}{dz}\exp(2ikz)\,dz \tag{11}$$

Thus, in this limit the reflectivity is simply related to the Fourier transform of the derivative of the scattering length density profile.[16] It is easy to see that the contribution of a diffuse interface of half-width D disappears for wavevectors $k > 1/D$; thus at high k the reflectivity is solely determined by any sharp jumps in the scattering length density; that is

$$\lim_{k\to\infty} R = \frac{\pi^2}{k^4}\sum_i \{\delta(b/V)\}_i^2 \tag{12}$$

where the $\delta(b/V)$ are the magnitudes of the jumps in scattering length density. Thus from high-k data one is able to extract parameters such as the surface volume fraction essentially independently of any model.

This approximation is only valid for low reflectivities and high values of k_0 and is not in general useful for quantitative analysis of results, but it often offers useful

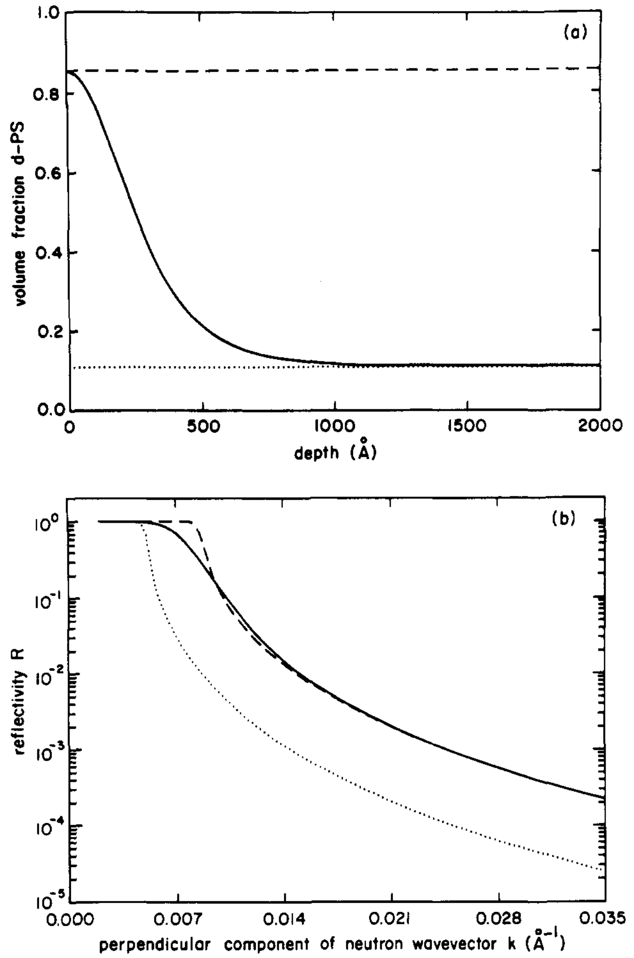

Figure 3. The importance of tunneling for neutron reflectivity measurements. (a) A schematic adsorption profile (solid line) which presents a potential barrier for incoming neutrons. (b) The neutron reflectivity R as a function of the perpendicular component of the neutron wavevector k predicted for the adsorption profile in (a) (solid line). The dotted and dashed lines show, for comparison, neutron reflectivities predicted for a uniform layer of the same bulk volume fraction as the adsorption profile (dotted line) and for a uniform layer of the same surface volume fraction as the adsorption profile (dashed line).

qualitative guidance in the design of experiments. However, it offers no help in understanding the situation in which there is a finite region of high scattering length density such that $[k^2 - 4\pi(b/V)] < 0$. Such a case is realized if a high scattering length density material such as deuterated polystyrene is adsorbed at a surface or an interface. In this situation the neutron propagates as an evanescent wave within the region; yet if the region is relatively thin, the reflectivity is less than unity because the neutrons can tunnel through the potential barrier—one has frustrated total reflection. The tunneling occurs with higher probability where the barrier is thinner and is a very sensitive function of the thickness and height of the barrier at a given k.

Thus measurements of the reflectivity just beyond the critical k are influenced greatly by small changes in the composition profile of the high scattering length density species. This point is illustrated in Figure 3. The reflectivity of the adsorption profile shown in Figure 3a as a solid line is shown as the solid line in Figure 3b. At high k the reflectivity is the same as that from a uniform layer of the same composition as the surface composition of the adsorption profile (dashed line), as predicted by eq 12. The adsorption profile reflectivity begins to deviate from unity at the same value of k as a uniform profile with the same bulk composition (dotted line), but instead of the reflectivity rapidly falling off at a sharp critical k, there is a gentle reduction in reflectivity due to increased tunneling through the barrier. Of course this type of information is only available if the experiment has been designed so it is the high scattering length density material that is adsorbed to the surface or interface. Additionally, a relatively low scattering length density substrate must be chosen so that the tunneling information is not masked by total reflection from the substrate.

In practice, NR data are analyzed by assuming a trial profile which seems physically reasonable, calculating the reflectivity of this model profile using the LAYERS algorithm, and then refining parameters to achieve good agreement between simulation and experimental data. This optimization may be done either manually or using a least-square routine.

Although such a procedure allows accurate refinement of model parameters, there remains the danger that a fundamentally wrong model has been chosen. Formally this problem is related to the mathematical impossibility of inverting reflectivity curves to give the potential when phase information is lacking and reflectivities are known only in a limited k range. In this experiment, for example, one might be able to get a reasonable fit to reflectivity data by assuming that segregation has taken place to the surface rather than to the silicon interface.[17] Our major defense against this type of misinterpretation is provided by the forward recoil spectrometry data. This technique provides a direct space–concentration profile, albeit with poor depth resolution (~800-Å fwhm). In effect this profile provides us with a crude model, whose parameters can then be refined with confidence using the NR data within limits set by the constraints provided by FRES data.

In this experiment we have additional evidence that segregation has taken place to the silicon interface rather than to the surface. In the foregoing no account has been taken of either absorption or incoherent scattering; for these hydrogenous materials on a silicon substrate absorption is not important, but incoherent scattering due to hydrogen is. We can include these effects by allowing the scattering length density to be complex; the imaginary part is given by $b_i = \sigma_T/2\lambda$, where σ_T is the total cross section and λ is the neutron wavelength.[18] If $b_i \ll b_r$ the Fresnel reflectivity is hardly affected by the imaginary term. Consider, however, a system comprising a substrate coated with a single film. The total reflectance of the system is given by

$$r = \frac{r_{1,2} + r_{2,3}\exp(2ik_2d_2)}{1 + r_{1,2}r_{2,3}\exp(2ik_2d_2)} \qquad (13)$$

where $r_{2,3}$ is the reflectance of the film/substrate interface and $r_{1,2}$ is the reflectance of the air/film interface. Assume that $|r_{1,2}| < |r_{2,3}|$. When k has the critical value k_{c1} for the first interface, the resulting reflectivity is unperturbed by b_i. For values of k only slightly larger than k_{c1}, $|r_{1,2}|$ becomes small compared to unity, while $|r_{2,3}| = 1$; in the first approximation the reflectivity is given by

$$r = r_{2,3}\exp[2i\sqrt{k^2 - 4\pi(b/V)}\,d_2] \times \exp\left[-\frac{(b_i/V)d_2}{\sqrt{k^2 - 4\pi(b/V)}}\right] \qquad (14)$$

The reflectivity beyond the first critical value is damped, because the neutrons are absorbed or incoherently scattered in traversing the film. Of course this damping would

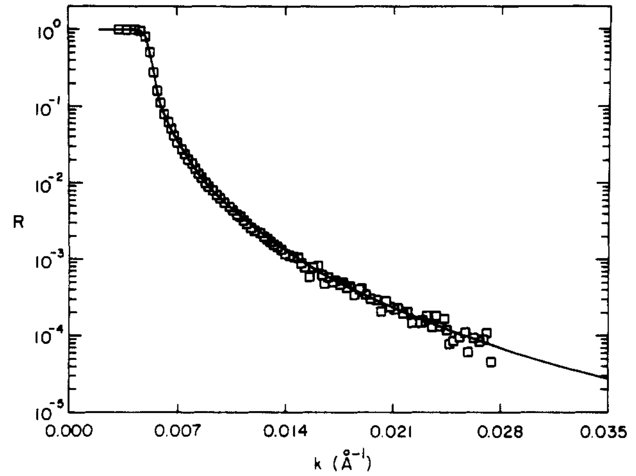

Figure 4. Neutron reflectivity R as a function of the perpendicular component of the neutron wavevector k for a blend of 0.133 volume fraction end-functionalized deuterated polystyrene with hydrogenated polystyrene of molecular weight 575 000 as cast. The solid line is the prediction of the Fresnel expression (eq 5).

not be present if $|r_{1,2}| > |r_{2,3}|$.[19] In our case the film is mostly protonated; the total cross section for light hydrogen is 80 × 10^{-24} cm^2 for 4-Å neutrons, mostly due to incoherent scattering, from which $b_i = 1 \times 10^{-15}$ cm, against $b_r = -374 \times 10^{-15}$ cm. If the end-functionalized polystyrene segregates to the silicon, the reflectivity of the substrate/film interface will be greater than the film/air interface. Thus above the critical k for the air/polymer interface, but below the critical k for the polymer/substrate interface (with its strongly reflecting adsorbed deuterated polystyrene layer), the reflectivity will be less than unity.

4. Results

Figure 4 shows the neutron reflectivity R as a function of the perpendicular component of the neutron wavevector k for an unannealed blend of 0.133 volume fraction of the end-functionalized dPS with hPS. The solid line shows the expected reflectivity for a uniform film of that volume fraction given by the Fresnel formula, eq 5. The agreement between the experimental and the predicted reflectivity is excellent, showing that the unannealed film is indeed uniform.

Figure 5 shows the neutron reflectivity R as a function of the perpendicular component of the neutron wavevector k for a similar film of the same starting volume fraction (0.133) after annealing in vacuum for 25 h at 184 °C. The much greater value of the reflectivity, compared to the uniform film (Figure 4), indicates a substantial segregation of the deuterated component. Figure 6 shows a low-resolution direct space depth profile obtained by forward recoil spectrometry, showing substantial segregation to the silicon interface. These data also show that the actual bulk volume fraction is $\phi_\infty = 0.11$; depletion of the bulk volume fraction has occurred. The detailed shape of the neutron reflectivity curve near the critical edge (inset to Figure 5) shows an anomaly which confirms that the segregation is at the silicon interface. There is a pronounced dip in the reflectivity at a value of k which corresponds to the critical k for reflection from a vacuum/11% dPS interface. This is due to the loss of neutron intensity by incoherent scattering as discussed above. If the dPS were segregated at the surface there would be no penetrating traveling wave which could undergo incoherent scattering until a higher value of k were reached.

The solid line is a fit to the data, based on the concentration profile shown in Figure 7. The reflectivity expected for this model profile was calculated using the multilayer algorithm[14] (eqs 5 and 7–9), with a complex scattering length density to include the effects of incoherent scattering. The functional form of the profile is given by

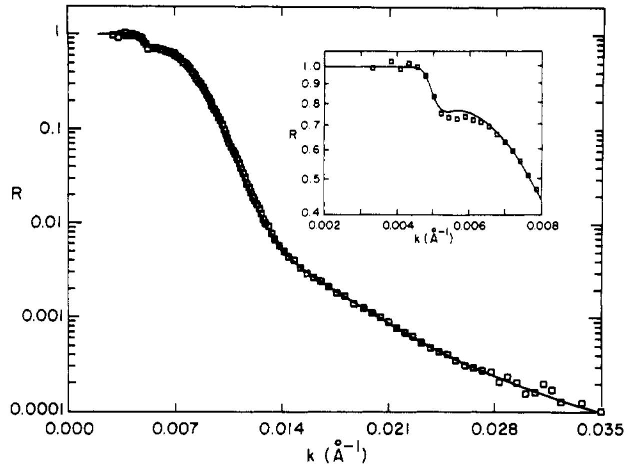

Figure 5. Neutron reflectivity R as a function of the perpendicular component of the neutron wavevector k for a blend of 0.133 volume fraction end-functionalized deuterated polystyrene with hydrogenated polystyrene of molecular weight 575 000 after annealing for 20 h at 184 °C. Inset: enlargement of the region near the critical edge.

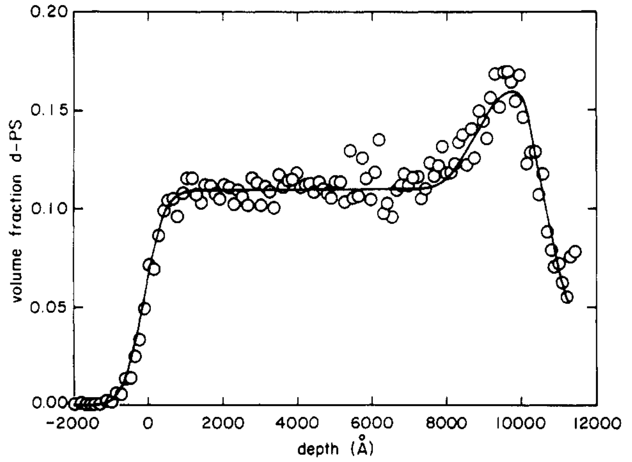

Figure 6. Direct space depth profile for a blend of 0.133 volume fraction end-functionalized deuterated polystyrene with hydrogenated polystyrene of molecular weight 575 000 after annealing for 20 h at 184 °C, as revealed by forward recoil spectrometry. The solid line is a fit assuming a bulk volume fraction of end-functionalized deuterated polystyrene of 0.11 and an interfacial excess of 203 Å.

$$\phi(z) = \frac{1}{2}\left[(\phi_1 + \phi_\infty) - (\phi_1 - \phi_\infty)\,\mathrm{erf}\left(\frac{z - \lambda_0}{\lambda}\right)\right] \qquad z \geq \lambda_{\max} \quad (15a)$$

$$\phi(z) = \phi_m - (\phi_m - \phi_0)\left(1 - \left(\frac{z}{\lambda_{\max}}\right)\right)^2 \quad z \leq \lambda_{\max} \quad (15b)$$

where $\phi_m = \phi(\lambda_{\max})$.

This empirical function allows a reasonable fit (normalized $\chi^2 \approx 3.5$) to be obtained by varying five parameters (the bulk volume fraction is obtained from the FRES measurements and is in any case consistent with the known starting volume fraction, the total thickness of the film, and conservation of material). In contrast, if one attempts to fit a simpler profile based on an error function with no maximum (with three variable parameters), the normalized

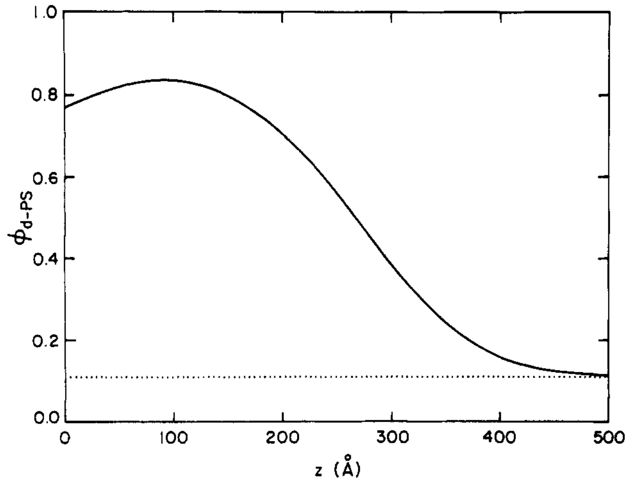

Figure 7. Concentration profile which provides the best fit to the data shown in Figure 5.

χ^2 is 75. At large k one expects, as shown in eq 6, that k^4R should tend toward a constant value, proportional to the sum of the squares of the jumps in scattering length density profile.[16] Thus a sensitive determination of the interface volume fraction may be made which is not dependent on an assumed model profile. The data at lower k indicates that the potential barrier is higher than would be obtained by a volume fraction profile that monotonically decreases from the interfacial volume fraction determined by the high-k data. Hence we believe that the maximum in volume fraction is a real feature.

Reflectivity curves were obtained for annealed films of end-functionalized dPS in blends with hPS of molecular weight 575 000 with other starting compositions and are shown in Figure 8a–c. In each case the solid line represents the best fit obtained by varying the parameters of the model represented by eq 15. Normalized χ^2 values for the fits are in the range 3–6.

One check on the validity of these profiles is to compare the integral interface excess, defined as

$$z^* = \int dz\,(\phi(z) - \phi_\infty) \qquad (16)$$

as determined experimentally using forward recoil spectrometry with the values found by integrating the profiles. These two measures of z^*, which are shown in Figure 9 as a function of the volume fraction of end-functionalized dPS in the bulk, are in excellent agreement, adding confidence that the procedure we have used to fit the neutron reflection data are reasonable.

The best fit parameters for the samples are summarized in Figures 10 and 11. Figure 10 shows both the interface volume fraction and the volume fraction at the maximum as determined by the NR fits as a function of the bulk volume fraction of dPS after annealing, as determined by FRES; the dotted line represents no segregation. Figure 11 shows the position of the offset of the error function and the width parameter of the error function. The latter is rather insensitive to the bulk volume fraction, while the former gradually decreases with decreasing bulk volume fraction, and thus interface volume fraction, of end-functionalized polymer.

5. Discussion

Since similar mixtures of dPS and hPS where the dPS is not end-functionalized show no discernible segregation to the Si interface, it seems obvious that the dPS in the segregated layer is tethered by its end-functional group to the interface. While the idea of end-group tethering has been much discussed for the situation when the grafted chains are immersed in solvent,[20–29] less attention has been given to the melt case,[30–33] but the ideas developed for solvents may be extended to the melt case. A scaling analysis due to de Gennes[30] and developed by Leibler in the context of block copolymers[34] identifies the various regimes. Consider polymer chains of degree of polymerization N attached by one end to a surface with a dimensionless grafting density σ defined as the product

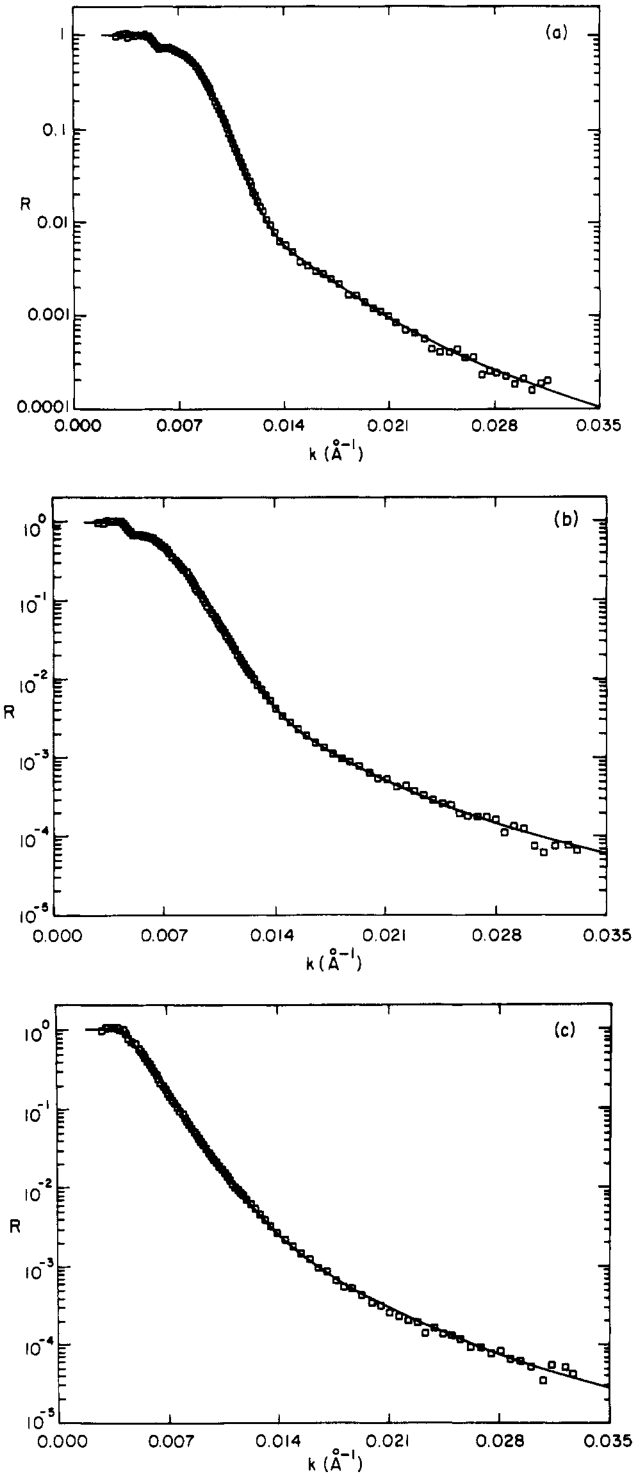

Figure 8. Neutron reflectivity R as a function of the perpendicular component of the neutron wavevector k for blends of end-functionalized deuterated polystyrene with hydrogenated polystyrene of molecular weight 575 000 after annealing for 20 h at 184 °C. The actual bulk volume fractions of dPS after annealing, as determined by FRES, are (a) 0.16, (b) 0.07, and (c) 0.03.

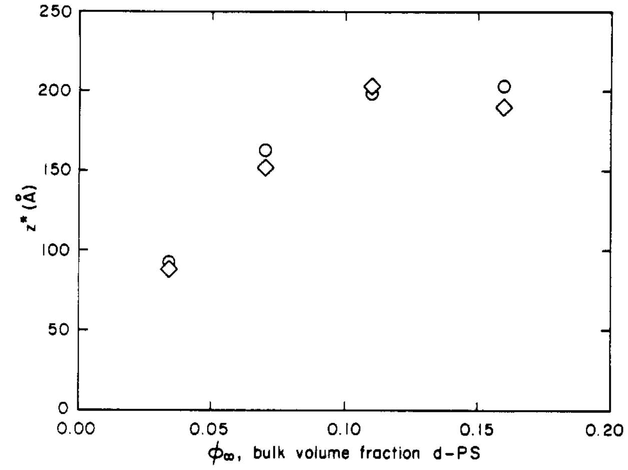

Figure 9. Integral interfacial excess z^* determined by forward recoil spectrometry (diamonds) and from the concentration profiles determined by neutron reflectometry (circles) shown in Figures 7 and 8 versus the bulk volume fraction of dPS.

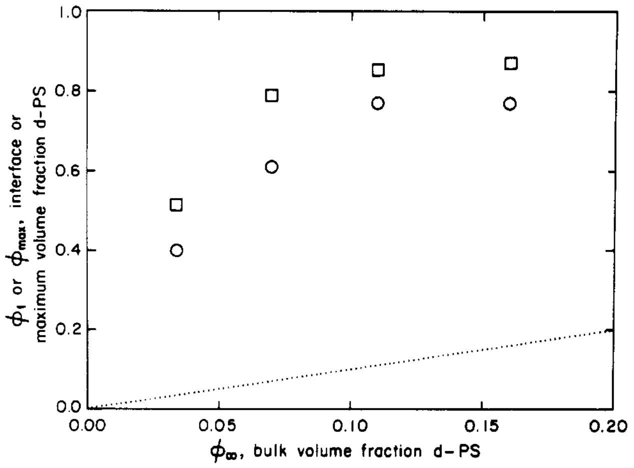

Figure 10. Volume fraction of the end-functionalized dPS at the interface with the silicon substrate (circles) and the maximum volume fraction of dPS (squares), as revealed by the neutron reflectivity experiments. Dotted line represents no segregation.

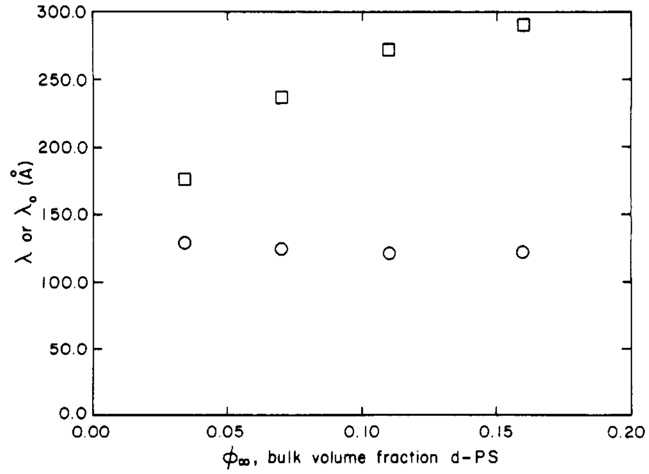

Figure 11. Best fit parameters for the neutron reflectivity profiles: (a) λ_0 offset of the error function (squares); (b) λ width parameter of the error function (circles).

of the area b^2 occupied by one chain segment at the interface and the number of end-anchored chains per unit area ν_i. These chains are surrounded by a matrix of polymer chains of degree of polymerization P (Figure 12). At low values of the surface excess, one expects each chain

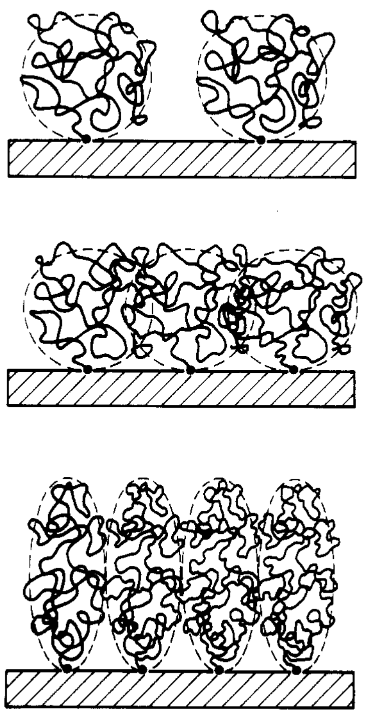

Figure 12. End-grafted polymers in solutions and melts.

to be essentially independent of its neighbors, forming a "mushroom"; as the interfacial areal density becomes larger the anchored chains start to interact and form a "brush", in which the chains are stretched in an attempt to minimize their unfavorable interactions. In a good solvent (which for a melt corresponds to the case $P < N^{1/2}$) neighboring chains start to interact unfavorably and become significantly stretched as soon as the chains physically overlap; thus we expect the "mushroom–brush transition" to occur when the condition $\sigma > N^{-6/5}$ is satisfied. The size of the mushroom is essentially the radius of gyration of the grafted polymer. In the brush, however, the disposition of the brush, and in particular its height, is given by a balance between stretching energies and excluded volume interactions between the chains of the brush; one expects the height of the brush to be significantly greater than the size of the radius of gyration. Simple scaling arguments lead to a prediction that the height scales as $L \sim Na\sigma^{1/3}$, where a is the statistical step length. The essential difference between melts and solutions lies in the screening out of excluded volume. The effective excluded volume parameter scales as $1/P$, where P is the degree of polymerization of the "solvent" chain; this means that for $P > N^{1/2}$ chains may physically interpenetrate without substantially interacting, and the transition to the strongly stretched state occurs when the condition $\sigma > PN^{-3/2}$ is satisfied. Thus there is an additional regime, the "screened brush" regime, where the chains interpenetrate but are not strongly stretched. As the degree of polymerization of the matrix chains, P, is increased above the degree of polymerization of the brush chains, N, one expects the P chains to be progressively expelled from the brush, leading to a "dry brush regime". In this regime the applicability of simple scaling arguments becomes delicate; the P chains have to be distorted from their Gaussian conformations in order to maintain constant density, and this additional free energy may become important. However, detailed self-consistent field calculations[32] in fact reveal that there is a universal "dry brush" regime for coverages $\sigma > N^{-1/2}$ for which the profiles become insensitive to the solvent molecular weight. In this limit the height of the polymer brush scales as $L \sim Na\sigma$, that is as if the brush formed

Table I
Parameters of the Interfacial Segregation Profile

bulk volume fraction ϕ_∞	interfacial volume fraction ϕ_0	interfacial integral excess z^*, Å	adsorption energy β, kT	interfacial field μ_i, Å	interfacial energy difference $\mu_i kT/b^3$, mJ/m^2	normalized integral excess z^*/R_g	normalized grafting density σ
0.16	0.77	203	4.12	0.13	0.47	1.51	0.0150
0.11	0.77	199	4.24	0.11	0.40	1.48	0.0147
0.07	0.61	163	4.30	0.12	0.43	1.22	0.0122
0.03	0.40	92	3.94	0.07	0.25	0.69	0.0069

an unmixed layer at the interface. However, it must again be stressed that the concentration profile of brush monomers is not expected to be close to a step function; substantial penetration of the "dry brush" by the matrix chains still takes place.

There have been two main approaches to calculating interfacial composition profiles of such grafted chains, both essentially based on the self-consistent field theory for calculating polymer properties.[35] One approach[27-29,33,36] has used the correspondence between the self-consistent field theory of polymers and Schrödinger's equation to argue that brushes in their strongly stretched condition represented an analogue to the classical limit of Schrödinger's equation. Thus an analytic expression for the self-consistent field can be derived. This can be converted into a segment density profile with suitable assumptions about the free energy of mixing.

In the present case, however, there are several drawbacks to this analytical approach. The numerical values of grafting density σ for all our samples (Table I) lie between 0.006 and 0.015, well within the screened brush regime and far short of the value (0.050) that our values of N and P mark as the boundary of the stretched brush regime. The strong stretching necessary for the classical limit of the Schrödinger equation to be valid is therefore not achieved. Furthermore, the analytical approach assumes that only the segment density of the grafted chains is important in determining the free energy of the brush. While this assumption is reasonable when the grafted chains are dissolved in low molecular weight solvent, it is questionable when the matrix chains are high molecular weight homopolymers. For high molecular weight matrices, the constaint of nearly constant segment density will impose an entropic penalty on the matrix chains at the interface that is not included in the analytical approach.

An alternate approach is to solve the self-consistent field equations numerically.[24-26,32,37] The disadvantage of this approach (besides perhaps a certain loss of transparency) is that the calculations are long and take much computer time; however, it has the advantage that no further approximations are involved beyond the basic mean field framework. The numerical solution scheme we use to obtain such self-consistent field (SCF) predictions to match with our data has been discussed in detail elsewhere.[32]

This numerical scheme allows one not only to calculate the self-consistent field composition profile for a grafted polymer layer of a given grafting density but also to determine the equilibrium grafting density in terms of the strength of the interaction between the adsorbing chain end and the interface. This interaction strength can be characterized by a parameter β, such that $kT\beta$ is the net free energy decrease associated with the confinement of an adsorbing end to within a distance δ of the interface:

$$\beta = \chi_e^{\,b} - \chi_e^{\,s} + 1.1 \ln (\delta/R_g) \qquad (17)$$

Here $kT\chi_e^{\,b}$ is the free energy of interaction of the end group with the bulk polymer, $kT\chi_e^{\,s}$ is the free energy of interaction of the end group with the interface, and the logarithmic term is the entropic penalty associated with confining the end group to within a distance δ of the interface; R_g is the radius of gyration of the polymer chain. In the calculations one varies $\chi_e^{\,b} - \chi_e^{\,s}$ in order to reproduce the observed values of coverage. The values of β we quote are then obtained by adding to this value the (negative) value of the logarithmic term calculated for the particular value of δ used in the calculation. Thus although the value of $\chi_e^{\,b}$ needed to match the observed coverage depends on the lattice unit used in the calculation, the value of β obtained is the physically meaningful driving force for adsorption, free of lattice artifacts. Figure 13 shows the experimentally determined composition profile for the 0.16 bulk volume fraction sample, compared with the SCF profile calculated by varying the sticking free energy β in order to reproduce the observed coverage. One sees that the height of the brush and the general shape of the decay from the brush to the bulk polymer are well accounted for. However, the maximum observed in the experimental profile is not reproduced by this version of the SCF theory; the theoretical profile always decays monotonically from the wall into the bulk. It is also worth mentioning that the maximum appears not to be an artifact of the particular end group used; our recent experiments using end-functionalized dPS chains with several different end groups, e.g. OH and OLi, show very similar maxima.

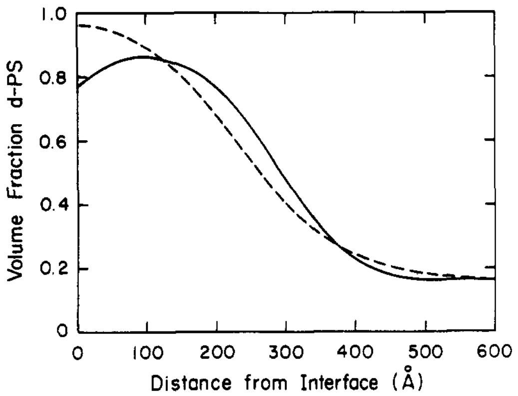

Figure 13. A comparison of the measured profile (solid line) for a blend of end-functionalized deuterated polystyrene with hydrogenated polystyrene of molecular weight 575 000 after annealing for 20 h at 184 °C (actual bulk volume fraction after annealing = 0.16) with the theoretical profile (dashed line) calculated using the self-consistent field theory for polymer melts for a value of the adsorption parameter β = 3.46.

One important assumption of this version of SCF theory is that there is no difference between the interaction of the PS homopolymer segments of the matrix and the dPS polymer segments of the end-functionalized polymer with the silicon; i.e., the wall is neutral for the various PS and dPS segments. In this regard it is useful to realize that at our grafting densities only a minute fraction of the silicon interface is occupied by the end groups; most of the area of the interface is occupied by contacts between segments of the various polymers and the silicon. If, in the absence of the end groups, one or other of the species would adsorb to the wall, a different boundary condition at the wall would have to be applied. Such a difference in interfacial

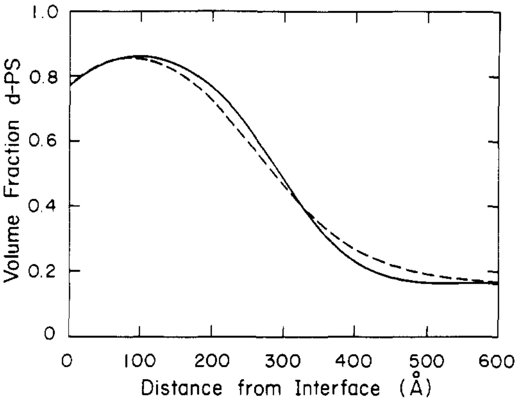

Figure 14. A comparison of the measured profile (solid line) for a blend of end-functionalized deuterated polystyrene with hydrogenated polystyrene of molecular weight 575 000 after annealing for 20 h at 184 °C (actual bulk volume fraction after annealing = 0.16) with the theoretical profile (dashed line) calculated using the self-consistent field theory for polymer melts for a value of the adsorption parameter $\beta = 4.12$ and a value for the interfacial field $\mu_i = 0.13$ Å.

energies of the chain segments may be included in the SCF calculations. The strength of the interaction may be characterized by the interfacial field parameter μ_i, which is proportional to the change in free energy of the system when a segment of dPS at the interface is replaced by a segment of hPS; the difference in interfacial energies between the two components would be given by $\mu_i kT/b^3$, where b^3 is the volume of a polymer segment. Figure 14 shows a comparison of the experimentally determined composition profile for the 0.16 bulk volume fraction sample with the SCF profile obtained by varying both the sticking energy β and the interfacial field μ_i to match the observed coverage and interfacial volume fraction. The value of μ_i used is 0.13 Å ($\mu_i kT/b^3 = 0.47$), representing a preference of the hPS over dPS segments for the Si; this is about 4 times the magnitude and the opposite sign of the isotopic differential surface energy between hydrogenated polystyrene and deuterated polystyrene deduced from surface segregation experiments.[4] In independent experiments we have found the hydrogenous component of another H/D polymer blend has a slight preference for the interface with silicon.[38]

Figure 15 shows comparisons between the experimental profiles for 0.11, 0.07 and 0.03 bulk volume fractions, together with the values for β and μ_i which best matched the observed coverages and interfacial volume fractions. The best fit values are listed in Table I. Figure 16 shows the observed interfacial volume fractions compared to the values predicted on the basis of the mean values of β and μ_i. Figure 17 shows the normalized surface excess of end-functionalized polymer (normalized by the radius of gyration (134 Å) of the end-functionalized dPS chain) as revealed by neutron reflectivity together with the values predicted on the basis of the mean values of β and μ_i plotted as a function of bulk volume fraction ϕ_∞. The agreement between the predicted and experimental parameters seems reasonable, especially in the light of some considerable uncertainties as discussed below.

The first caveat to be mentioned is that we have really no way of determining whether our experimental concentration profiles as measured by neutron reflectometry or any other experimental technique truly represent an equilibrium state; the profiles predicted by the SCF theory are, of course, equilibrium ones. In order for our profiles to qualify as equilibrium profiles, we must be able to assure ourselves that the end groups are mobile enough to adjust their spacing on the interface so as to approach the equilibrium spacing as more and more ends adsorb. While we can predict, on the basis of the diffusion coefficient of dPS, that 20 h is ample time to achieve equilibrium in the bulk (and neutron reflection measurements on a sample annealed for 56 h show very little difference from that annealed for 20 h), until now we have had no method to follow this lateral rearrangement along the interface. Since one might imagine that the mobility of the end groups would be severely restricted at the interface, this question remains open.

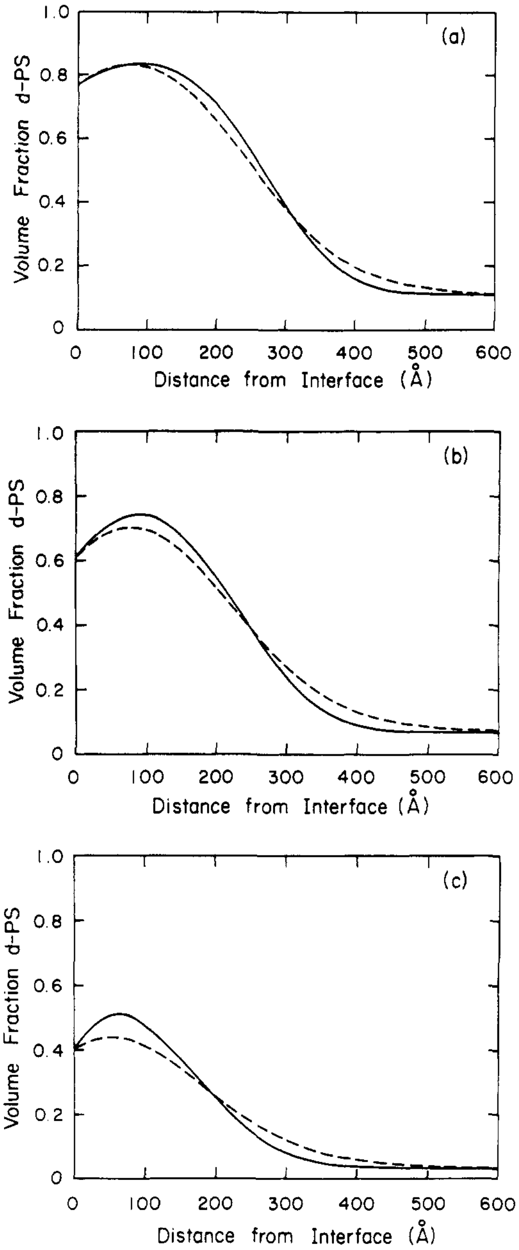

Figure 15. Comparisons of the measured profiles (solid lines) for blends of end-functionalized deuterated polystyrene with hydrogenated polystyrene of molecular weight 575 000 after annealing for 20 h at 184 °C with the theoretical profile (dashed line) calculated using the self-consistent field theory for polymer melts: (a) 0.11 actual bulk volume fraction, adsorption parameter $\beta = 4.24$, interfacial field $\mu_i = 0.11$ Å; (b) 0.07 actual bulk volume fraction, adsorption parameter $\beta = 4.30$, interfacial field $\mu_i = 0.12$ Å; (c) 0.03 actual bulk volume fraction, adsorption parameter $\beta = 3.94$, interfacial field $\mu_i = 0.07$ Å.

The second point is that we have no direct evidence that the values of μ_i needed to produce the maximum are reasonable. While experiments are underway to check this point, it is worth at least considering that the failure

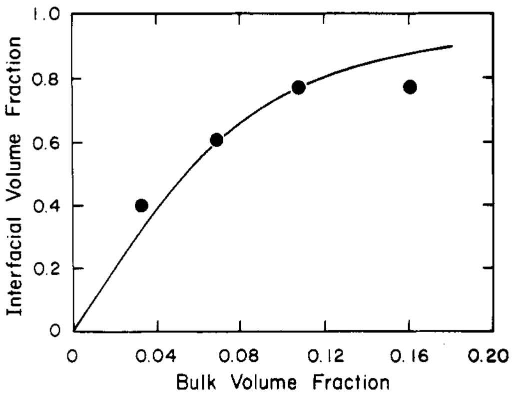

Figure 16. The observed interfacial volume fractions (filled circles) of the end-functionalized deuterated polystyrene as a function of actual bulk volume fractions compared with the prediction of self-consistent field theory with adsorption parameter $\beta = 4.15$ and interfacial field $\mu_i = 0.11$ Å.

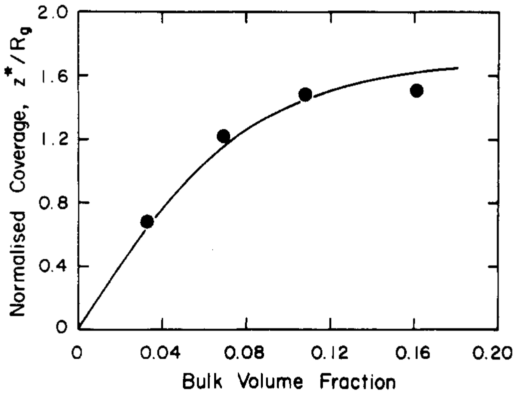

Figure 17. The observed integrated interfacial excess of the end-functionalized deuterated polystyrene, as revealed by neutron reflectivity (filled circles), as a function of actual bulk volume fractions compared with the prediction of self-consistent field theory with adsorption parameter $\beta = 4.15$ and interfacial field $\mu_i = 0.11$ Å.

of the mean field theory to predict the maximum for $\mu_i = 0$ might be due to a breakdown of the basic mean field approximation, i.e., replacement of the actual chain statistics by the appropriate averages. The averaged quantities in the theory are distribution functions which describe the probabilities that different portions of a polymer chain are located in specified regions of space. Polymer chain connectivity is taken into account through relationships between the averaged probabilities. A more rigorous approach would be to avoid this preaveraging scheme by consideration of an ensemble of completely connected chains. The effects of the preaveraging scheme on the polymer chain statistics are known to be negligible for homogeneous blend systems, where the chain statistics as probed by scattering methods are in good agreement with the mean field prediction of Gaussian chains.[39] (The mean field approximation is referred to as the random phase approximation in this context.) Nevertheless, the perturbation to these statistics in the presence of the strong spatial inhomogeneities induced by the interface may be responsible for some of the results which we see here. Unfortunately, calculation of the adsorbed polymer profile without resorting to the mean field approximation is an enormously complex problem. Within the context of existing theory, we believe our interpretation of the maximum in terms of μ_i is the best possible.

A distinction must be made between our results, which are valid for polymers adsorbed from a matrix of high molecular weight polymer, and similar results for adsorption from a solution of the polymer in a small-molecule solvent. From a theoretical standpoint, adsorption from solution has been studied in great detail, as noted above, because of the direct relevance of this problem to the polymeric stabilization of colloidal dispersions. One is tempted to apply such theories to experimental results for melts, as indeed has been done in a recent study.[40] There are, however, fundamental differences between the two cases which lead to dramatic differences in the types of profiles which are obtained. The simplest way to illustrate the difference between these two types of adsorption is to consider a grafted polymer chain as a one-dimensional random walk at an impenetrable wall. Di Marzio and McCrackin[41] considered exactly this problem more than 25 years ago, for the general case where polymer chain segments may have an adsorption energy to the wall. When the adsorption energy is zero, the maximum in the polymer volume fraction is removed from the wall by a distance approximately equal to the radius of gyration of the polymer chain.

The physical origin of the maximum away from the wall can be understood in terms of the entropic penalty associated with sharp gradients in polymer concentration, a penalty which arises from the polymer chain connectivity. Low molecular weight solvent molecules, which can be imagined to occupy the rest of the half-space of Di Marzio and McCrackin's problem, do not suffer this entropy penalty. The volume immediately adjacent to a sharp interface can be more easily filled with solvent molecules than with polymer chain segments. This situation changes when the small-molecule solvent is replaced by a high molecular weight polymer (i.e., with the matrix chains). Now the same entropic penalty associated with sharp gradients in the concentration profile of the adsorbed polymer applies to the matrix polymer as well. A constant-density constraint must be introduced; one cannot simply assume that the volume not taken up by the grafted polymer will be taken up by a small-molecule solvent. This constraint introduces an effective attractive potential adjacent to the wall which "pulls" material into the interfacial region. One must therefore compare the self-consistent mean field results with those of Di Marzio and McCrackin in the presence of an attractive potential at the wall, which indeed show monotonically decreasing polymer profiles for attractive potentials which are greater than some critical value. This attractive potential is determined self-consistently in the SCF theory which we have used and is not an adjustable parameter. The value of this potential is such that, in the absence of the preferential interaction characterized by μ_i, the profiles are monotonically decreasing. Introduction of a preferential affinity for the matrix chains at the interface through μ_i decreases the effective attractive potential for the adsorbed polymer segments at the interface, resulting in the reappearance of the maximum away from the interface.

Finally, we should discuss briefly why such an end group, a few units of butadiene terminated by a trimethylsilicon, should adsorb so strongly to the silicon interface. Separate control experiments, using FRES, have shown that there is little difference in adsorption when the trimethylsilicon is removed from the short butadiene block (by terminating that block with H) whereas there is little, if any, adsorption when the dPS block is terminated with H. All these chains had the same initiator, *sec*-butyllithium, and were synthesized in the same batch before being divided into three parts to be terminated differently. Thus it appears that the terminating end group drives the segregation, and what drives that end group to adsorb is the short butadiene segment. While we are unable to speculate directly on the chemical mechanisms involved, strong attraction of butadiene segments to silicon-containing substrates is consistent with experiments carried out by Gent and coworkers[42] on the adhesion between various glass surfaces and polybutadiene. They found strong adhesion of polybutadiene to glass, almost as strong as when the glass had been treated with a vinylsilane which formed a covalent bond to the polybutadiene and nearly 2 orders of magnitude stronger than the adhesion to glass treated with ethylsilane.

6. Conclusion

In conclusion, then, we have demonstrated that a rather small end group on a polymer chain can cause substantial interfacial segregation of such chains from a blend with normally terminated polymer. This strong segregation is another consequence of the weak entropy of mixing that is the important feature of blend thermodynamics. It follows from this fact that segregation is stronger when the molecular weight of the matrix is large.

Neutron reflectivity measurements allow us to probe the segment density profile of such end-adsorbed chains with unparalleled sensitivity. We find that the adsorbed layer stretches out a distance which is a few times the radius of gyration of the polymer and that its interface with the unadsorbed polymer is rather broad. If such end-attached chains were to be used to modify adhesion at the interfaces between polymers and inorganic substrates, this broad interface would be expected to lead to good adhesion between the adsorbed and unadsorbed layers.

Agreement with the predictions of self-consistent field theory is good; a single set of physically reasonable parameters gives good agreement with profiles measured for four different starting volume fractions of end-functionalized chains. An important feature of our data is the maximum which occurs near the wall. We believe that this is due to a slight difference in the interactions of deuterated and hydrogenated chains with the wall. This can be accounted for within the framework of the self-consistent field theory; the numerical value of the differential interfacial energy required to reproduce the observed effects is very small and is consistent with other observations. Future work is already in progress to make systematic measurements of adsorption profiles for a variety of end groups and for a number of solvent and brush molecular weight combinations.

Acknowledgment. This work was supported by the NSF–DMR Polymers Program (Grant DMR-8719123) at Cornell (R.A.L.J., L.J.N., and E.J.K.) and by the U.S. Department of Energy, BES–Materials Sciences, under Contract W31-109-ENG-28/at Argonne National Laboratory (G.P.F. and A.K.). At Cambridge R.A.L.J. is supported by a grant from ICI. We also used the central facilities of the Cornell Materials Science Center, which is supported by the NSF–DMR–MRL program, and the National Nanofabrication Facility, which is supported by the NSF under Grant ECS-8619049, Cornell University, and industrial affiliates.

References and Notes

(1) Napper, D. H. *Polymeric Stabilization of Colloidal Dispersions*; Academic Press: London, 1983.
(2) Russel, W. B.; Saville, D. A.; Schowalter, W. R. *Colloidal Dispersions*; Cambridge University Press: Cambridge, 1989.
(3) Bhatia, Q. S.; Pan, D. H.; Koberstein, J. T. *Macromolecules* **1988**, *21*, 2166.
(4) Jones, R. A. L.; Kramer, E. J.; Rafailovich, M. H.; Sokolov, J.; Schwarz, S. A. *Phys. Rev. Lett.* **1989**, *62*, 280.
(5) Green, P. F.; Christensen, T. M.; Russell, T. P.; Jerome, R. *Macromolecules* **1989**, *22*, 2189.
(6) Lipatov, Y. S.; Khramova, T. S.; Todosijchuk, T. T.; Gudova, E. G. *J. Colloid Interface Sci.* **1988**, *123*, 143.
(7) Jones, R. A. L.; Norton, L. J.; Kramer, E. J.; Composto, R. J.; Stein, R. S.; Russell, T. P.; Mansour, A.; Karim, A.; Felcher, G. P.; Rafailovich, M. H.; Sokolov, J.; Zhao, X.; Schwarz, S. A. *Europhys. Lett.* **1990**, *12*, 41–46.
(8) Morton, M.; Fetters, L. J. *Rubber Chem. Technol.* **1975**, *48*, 359.
(9) Doyle, B. L.; Peercy, P. S. *Appl. Phys. Lett.* **1979**, *34*, 811.
(10) Mills, P. J.; Green, P. F.; Palmstrøm, C. J.; Mayer, J. W.; Kramer, E. J. *Appl. Phys. Lett.* **1984**, *45*, 957.
(11) Shull, K. R.; Kramer, E. J.; Hadziioannou, G.; Tang, W. *Macromolecules* **1990**, *23*, 4780.
(12) Fermi, E.; Marshall, L. *Phys. Rev.* **1947**, *71*, 666.
(13) Squires, G. L. *Introduction to the Theory of Thermal Neutron Scattering*; Cambridge University Press: Cambridge, U.K., 1978.
(14) Born, M.; Wolf, E. *Principles of Optics*; Pergamon Press: Oxford, 1975.
(15) Russell, T. P. *Mater. Sci. Rep.* **1990**, *5*, 171.
(16) Landau, L. D.; Lifshitz, E. M. *Quantum Mechanics*, 3rd ed.; Pergamon Press: Oxford, 1977.
(17) Kramer, E. J.; Jones, R. A. L.; Norton, L. J. *Polym. Prepr.* (*Am. Chem. Soc., Div. Polym. Chem.*) **1990**, *31*, 75.
(18) This result may be derived by noting that the complex scattering length relates to a complex "optical" potential (eq 1) such that the real and imaginary parts of the neutron wavevector k_r and k_i are related by $k_i k_r = 2\pi(b_i/V)$ so that $k_i = (\lambda/\sin\theta)(b_i/V)$ (see: Lekner, J. *Theory of Reflection*; Martius Nijhoff: Dordrecht, 1987; 265). However, from the definition of the incoherent cross section σ_{inc}, $k_i = \sigma_{\text{inc}}/(2V\sin\theta)$, so since $\sigma_{\text{T}} \approx \sigma_{\text{inc}}$, $b_i \approx \sigma_{\text{T}}/2\lambda$.
(19) In fact the neutron density within the material is not zero even in the total external reflection case and so in principle some intensity will be lost even then, but as the evanescent wave penetrates only a distance of order 100 Å into the sample, incoherent scattering is insignificant.
(20) Dolan, A. K.; Edwards, C. F. *Proc. R. Soc. London, A* **1974**, *337*, 50.
(21) Dolan, A. K.; Edwards, S. F. *Proc. R. Soc. London, A* **1975**, *343*, 427.
(22) Alexander, S. *J. Phys.* (*Paris*) **1977**, *38*, 983.
(23) de Gennes, P.-G. *J. Phys.* (*Paris*) **1976**, *37*, 1443.
(24) Scheutjens, J. M. H. M.; Fleer, G. J. *J. Phys. Chem.* **1979**, *83*, 1619.
(25) Scheutjens, J. M. H. M.; Fleer, G. J. *J. Phys. Chem.* **1980**, *84*, 178.
(26) Cosgrove, T.; Heath, T.; van Lent, B.; Leermakers, F.; Scheutjens, J. *Macromolecules* **1987**, *20*, 1692.
(27) Milner, S. T.; Witten, T. A.; Cates, M. E. *Europhys. Lett.* **1988**, *5*, 413.
(28) Milner, S. T.; Witten, T. A.; Cates, M. E. *Macromolecules* **1988**, *21*, 2610.
(29) Milner, S. T.; Witten, T. A.; Cates, M. E. *Macromolecules* **1989**, *22*, 853.
(30) de Gennes, P.-G. *Macromolecules* **1980**, *13*, 1069.
(31) Brown, H. R.; Char, K.; Deline, V. R. *Macromolecules* **1990**, *23*, 3383.
(32) Shull, K. R. *J. Chem. Phys.* **1991**, *94*, 5723.
(33) Zhulina, E. B.; Borisov, O. V., to be published.
(34) Leibler, L. *Makromol. Chem., Makromol. Symp.* **1988**, *16*, 1.
(35) Edwards, S. F. *Proc. Phys. Soc. London* **1965**, *85*, 613.
(36) Pryamitsyn, V. A.; Borisov, O. V.; Zhulina, E. B.; Birshtein, T. M. *Modern Problems of Physical Chemistry of Solutions*; Donish and Leningrad University: Dushanbe and Leningrad, 1987.
(37) Hirz, S. J. M.S. Thesis, University of Minnesota, 1986.
(38) Jones, R. A. L.; Norton, L. R.; Kramer, E. J.; Bates, F. S.; Wiltzius, P.; *Phys. Rev. Lett.* **1991**, *66*, 1326. In this paper we see a slight preference on native silicon oxide for the hydrogenous component. In unpublished experiments we see the same preference at a silicon interface stripped of its oxide.
(39) de Gennes, P.-G. *Scaling Concepts in Polymer Physics*; Cornell University Press: Ithaca, NY, 1979; p 246.
(40) Zhao, X.; Zhao, W.; Rafailovich, M. H.; Sokolov, J.; Russell, T. P.; Kumar, S. K.; Schwarz, S. A.; Wilkins, B. J. *Europhys. Lett.* **1991**, *15*, 725.
(41) Di Marzio, E. A.; McCrackin, F. L. *J. Chem. Phys.* **1965**, *43*, 539.
(42) Ahagon, A.; Gent, A. N. *J. Polym. Sci., Polym. Phys. Ed.* **1975**, *13*, 1285.

Registry No. PS, 9003-53-6; neutron, 12586-31-1.